

Serotonin and childhood maltreatment interact to shape brain architecture and anxious avoidant behavior – a TPH2 imaging genetics approach

Congcong Liu^a, Lei Xu^a, Jialin Li^a, Feng Zhou^a, Xi Yang^a, Xiaoxiao Zheng^a, Meina Fu^a, Keshuang Li^a, Cornelia Sindermann^b, Christian Montag^{a,b}, Yina Ma^c, Dirk Scheele^d, Richard P. Ebstein^c, Keith M. Kendrick^a, Benjamin Becker^a

Affiliations

^a The Clinical Hospital of the Chengdu Brain Science Institute, MOE Key Laboratory for Neuroinformation, University of Electronic Science and Technology of China, Chengdu, China

^b Department of Molecular Psychology, Institute of Psychology and Education, Ulm University, Ulm, Germany

^c State Key Laboratory of Cognitive Neuroscience and Learning, IDG/McGovern Institute of Brain Research, Beijing Normal University, Beijing, China

^d Division of Medical Psychology, University of Bonn, 53105 Bonn, Germany

^e China Center for Behavior Economics and Finance, South Western University of Finance and Economics (SWUFE), Chengdu, China

Correspondence

Benjamin Becker, PhD
University of Electronic Science and Technology
Xiyuan Avenue 2006, 611731 Chengdu, China
Email: ben_becker@gmx.de

Abstract

Childhood maltreatment has been associated with emotional dysregulations and altered architecture of limbic-prefrontal brain systems engaged in emotional processing. Serotonin regulates both, developmental and experience-dependent neuroplasticity in these circuits. Central serotonergic biosynthesis rates are regulated by Tryptophan hydroxylase 2 (*TPH2*), and transgenic animal models suggest that *TPH2*-gene associated differences in serotonergic signaling mediate the impact of aversive early life experiences on a phenotype characterized by anxious avoidance. The present study employed an imaging genomics approach that capitalized on individual differences in a *TPH2* polymorphism (703G/T; rs4570625) to determine whether differences in serotonergic signaling modulate the effects of childhood maltreatment on brain structure and function and punishment sensitivity in humans (n = 252). Higher maltreatment exposure before the age of 16 was associated with increased gray matter volumes in a circuitry spanning thalamic-limbic-prefrontal regions and decreased intrinsic communication in limbic-prefrontal circuits selectively in TT carriers. On the phenotype level, the genotype moderated the association between higher childhood maltreatment exposure and higher punishment sensitivity. In TT carriers, the association between higher childhood maltreatment exposure and punishment sensitivity was critically mediated by increased thalamic-limbic-prefrontal volumes. The present findings suggest that childhood maltreatment shapes the neural organization of the thalamic-limbic-prefrontal circuits in interaction with individual variations in the *TPH2* gene to promote a phenotype characterized by facilitated threat avoidance, thus promoting early adaptation to an adverse environment.

Keywords amygdala, childhood maltreatment, punishment sensitivity, frontal cortex, serotonin

Introduction

Childhood maltreatment (CM) has been associated with strongly increased prevalence rates for psychiatric disorders and emotional dysregulations in adulthood. Converging evidence from animal and human studies suggest an association between CM and lasting alterations in the structural and functional organization of the brain, particularly in limbic systems engaged in threat and anxiety processing and, including the amygdala-hippocampal complex, and frontal systems engaged in emotion regulation (Teicher, Samson, Anderson, & Ohashi, 2016).

On the behavioral level, considerable variations in the long term sequelae of CM have been reported. For instance, longitudinal data suggests that whereas the majority of individuals with severe CM exhibits cognitive and emotional dysfunctions in adulthood, a significant minority remained unaffected (Sonuga-Barke et al., 2017), suggesting that innate factors such as genetic variations may influence the long-term sequelae of CM. Initial studies that combined candidate gene approaches with neuroimaging reported that specific single-nucleotide polymorphisms (SNPs) of genes associated with neuroplasticity and stress reactivity (brain derived neurotrophic factor, oxytocin receptor) may confer an increased susceptibility to the detrimental impact of aversive childhood experiences on the brain, i.e. pronounced reductions of limbic volumes following CM exposure (Dannlowski et al., 2016; van Velzen et al., 2016).

Serotonin regulates both, neuromaturation during sensitive periods as well as aversive learning-related neuroplasticity (Lesch & Waider, 2012), suggesting that innate differences in central serotonergic signaling may modulate the long-term effects of CM. Central serotonin biosynthesis is regulated by the rate-limiting enzyme tryptophan hydroxylase (*TPH*), with the second isoform *TPH2* being exclusively expressed in central serotonin neurons (Zhang,

Beaulieu, Sotnikova, Gainetdinov, & Caron, 2004). Individual differences in the *TPH2* encoding gene have been linked to variations in both, serotonin synthesis rates in limbic and prefrontal systems (Ottenhof, Sild, Lévesque, Ruhé, & Booij, 2018) and behavioral variations in emotional reactivity and regulation (Gutknecht et al., 2007).

Transgenic animal models that capitalized on the selective effects of the *TPH2* isoform on central serotonin (e.g. in a mouse model with a mutated *TPH2* knock-in human polymorphism resulting in reduced brain 5-HT levels) suggest that congenital *TPH2*-associated serotonergic deficiency mediates the impact of early aversive experiences on anxious behavior in adulthood (Sachs et al., 2013), possibly due to serotonergic modulation of synaptic plasticity in limbic-prefrontal circuits that underpin emotional learning (Lesch & Waider, 2012). In humans *TPH2* SNP rs4570625 (-703 G/T) variations modulate the impact of CM on emotional behavior, such that T-allele carriers exhibited increased threat attention in infancy (Forssman et al., 2014) and elevated stress-reactivity in adulthood (Mandelli et al., 2012). Despite accumulating evidence suggesting that *TPH2* genetics interact with early aversive experience to shape a phenotype characterized by anxious behavior, the brain systems that mediate this association have not been determined in humans.

To determine interactive effects of CM and the *TPH2* SNP rs4570625 (-703 G/T) polymorphism on brain structure and function and their relationship to anxious-avoidant behavior in adulthood a sample of healthy subjects (n = 252) underwent *TPH2* rs4570625 genotyping and brain structural and functional magnetic resonance imaging (MRI). CM exposure was retrospectively assessed by self-report, anxious behavior was assessed using a scale related to the Behavioral Inhibition System (BIS) (Gray, 1987). The BIS appears

particularly suitable given that it (1) specifically measures reactivity towards stimuli that are associated with a high probability of punishment and shapes anxious-avoidant behavior, and, (2) has been associated with the septo-hippocampal-amygdala system (Gray & McNaughton, 2000) and – in humans - prefrontal systems engaged in threat detection and emotion regulation (Fung, Qi, Hassabis, Daw, & Mobbs, 2019). Based on previous findings suggesting that (a) CM is associated with brain structural and functional changes in limbic-frontal circuits and that (b) *TPH2* genetic variations have been associated with serotonergic neurotransmission in these circuits (albeit with little direct evidence for the functional role of these SNPs, Ottenhof *et al.*, 2018) and (c) modulatory influence of brain serotonin levels on experience-dependent synaptic plasticity in limbic-frontal circuits, we hypothesized that, (1) the impact of CM on the structural and functional organization of limbic-prefrontal circuits varies as a function of *TPH2* rs4570625 genetic differences, and (2) CM-associated neuroplastic changes in this circuitry determine variations in anxious-avoidant behavior during early adulthood.

Methods

Participants

$N = 252$ healthy subjects (age range 18-29 years) from the Chengdu Gene Brain Behavior Project participated in the present study. Participants with current or a history of medical, physical, neurological, or psychiatric disorders or regular use of nicotine, alcohol, illicit substances, medication and MRI contraindications were not enrolled. The study was approved by the local ethics committee at the UESTC and was in accordance with the latest revision of the Declaration of Helsinki. Written informed consent was obtained from all participants.

Childhood experience, perceived stress and punishment sensitivity

Levels of CM exposure were assessed using the Childhood Trauma Questionnaire (CTQ) (Bernstein et al., 2003) which consists of 25 retrospective self-report items spanning five types of aversive childhood experiences. Following previous studies CTQ total score were used (Dannlowski *et al.*, 2016). Current stress (during the last months) was assessed using the Perceived Stress Scale (PSS) (Cohen, Kamarck, & Mermelstein, 1983). The Sensitivity to Punishment scale (SPS, Sensitivity to Punishment and Sensitivity to Reward Questionnaire, Torrubia, Avila, Moltó, & Caseras, 2001) was administered to assess individual differences in behavioral inhibition. Individuals with high punishment sensitivity experience high levels of anxiety and avoid potential dangers (Gray, 1987). Cronbach's α in the present sample demonstrated good internal consistency (0.847 CTQ; 0.834 PSS; 0.844 SPS). CTQ scores were non-normally distributed ($p < 0.001$, Shapiro-Wilk).

Genotyping

Genomic DNA was purified from buccal cells using a MagNA Pure96 robot (Roche Diagnostics, Mannheim), sample probes were designed by TIB MolBiol (Berlin, Germany). Genotyping was conducted by real-time polymerase chain reaction (RT-PCR) on a Cobas Z480 Light Cycler (Roche Diagnostics, Mannheim, Germany) according to the manufacturer's instructions.

MRI data acquisition and preprocessing

Brain structural and resting state functional MRI data were acquired on a 3 Tesla MRI system (GE 750) using standard acquisition protocols. After quality assessments of the data the

structural and functional data was preprocessed using validated procedures implemented in SPM12 (<http://www.fil.ion.ucl.ac.uk/spm/>). Details provided in **Supporting Information**.

Analysis of genotype x CM effects on brain structure and functional connectivity

Due to the non-normal distribution of CTQ scores, non-parametric permutation tests were employed to examine the effect of *TPH2* rs4570625genotype and CM on brain structure and function (Permutation Analysis of Linear Models, PALM) (Winkler, Ridgway, Webster, Smith, & Nichols, 2014). Gray matter (GM) volumes and functional connectivity maps were entered into a single full factorial model respectively, with genotype group as between-subject factor (TT vs. TG vs. GG). CTQ scores were entered as covariate (dimensional model), including the crucial CTQ times group interaction term. Age, gender, and education (for brain structure total intracranial volume, for resting state mean framewise displacement) were included as covariates. Based on the results of brain structural analysis we further explored whether regions showing *TPH2* genotype and ELS effects on brain structure additionally exhibit altered intrinsic functional interactions with other brain regions. To this end, seed-to-whole-brain voxel-wise connectivity maps were computed using standard protocols (Resting-State fMRI Data Analysis Toolkit; REST; <http://www.restfmri.net>, **Supporting Information**).

Statistical significance was determined using permutation-based inferences (10,000 permutations) and $p_{\text{FWE}} < 0.05$ using threshold-free cluster enhancement (TFCE) to control for multiple comparisons (within a gray matter mask, spm grey.nii > 0.3). In line with a previous study (Birn, Roeber, & Pollak, 2017), relative effects of CM and current stress on the brain were determined by recomputing the analyses and substituting CTQ with PSS scores.

Associations with anxious avoidant behavior

Associations between anxious avoidant behavior, CM and brain structure or function (extracted gray matter and functional connectivity estimates from 5mm-radius spheres centered at the peak coordinates of interaction clusters) were next examined. The moderation effect *TPH2* rs4570625 genotype on the association of CTQ with sensitivity to punishment was explored using a moderation analysis (PROCESS, Preacher & Hayes, 2004) testing whether the interaction between the predictor (CTQ) and moderator (genotype) could predict the dependent variable (SPS scores). Next associations between CM-associated brain structural or functional changes and the behavioral phenotype were explored using non-parametric correlation analyses (PALM, 10,000 permutations). Finally, a mediation analysis tested whether brain structural changes mediated effects of CM on an anxious avoidant behavior (punishment sensitivity) within genotype groups (bootstrapping with 10,000 permutations, bias-corrected 95% confidence intervals (CIs) to test the significance of indirect effects, Preacher & Hayes, 2008).

Results

Sample and genotyping

$N = 229$ right-handed Han Chinese participants (age $M = 21.55 \pm 2.31$, 115 females) were included in the analyses (exclusion see **Supplementary figure S1**). Genotyping for *TPH2* rs4570625 yielded $n = 71$ TT homozygotes, $n = 107$ GT heterozygotes, and $n = 51$ GG homozygotes (within Hardy-Weinberg Equilibrium $\chi^2_{(1)} = 0.735$, $p = 0.391$ and expected distribution for Han Chinese). Previous studies on the *TPH2* rs4570625 were mostly conducted in Caucasian populations with a rare occurrence of the T-allele, in contrast the present

distributions in Han Chinese allowed to separately examine GT and TT carriers. Genotype groups had comparable socio-demographics and CTQ scores ($ps > 0.36$), however, PSS scores were significantly higher in TT compared to GT carriers ($F_{(2, 226)} = 4.89, p = 0.008$, post-hoc $t_{(176)} = 3.10, p = 0.002$) (**Table 1**).

####table 1###

Interactive effects of TPH2 x CM on brain structure

No significant main effects of CM and genotype were found. Examining interactions of CM x genotype revealed effects in a broad thalamic-limbic-frontal network, including a cluster spanning the bilateral thalamus, parahippocampal gyrus, hippocampus, and amygdala ($k = 2609, p_{\text{FWE TFCE}} < 0.05$), a cluster spanning the bilateral ventromedial frontal cortex (vmPFC) ($k = 1575, p_{\text{FWE TFCE}} < 0.05$), and additional clusters located in the left dorsolateral prefrontal cortex (DLPFC) ($k = 201, p_{\text{FWE TFCE}} < 0.05$), right ($k = 335, p_{\text{FWE TFCE}} < 0.05$) as well as left ($k = 181, p_{\text{FWE TFCE}} < 0.05$) dorsal anterior cingulate cortex (dACC) (**Fig. 1**, details **Supplementary Table 2**). Post-hoc analyses by means of extracted parameter estimates from the significant interaction clusters revealed pronounced effects of CM on gray matter volume in TT homozygotes, whereas associations in GT heterozygotes and GG homozygotes failed to reach significance. In TT homozygotes, higher stress exposure during childhood specifically associated with increased gray matter volumes in the bilateral thalamic-limbic cluster, left dACC and dlPFC (all $ps < 0.05$ after Bonferroni correction, **Fig. 1**). Examination of correlation coefficients between the groups additionally revealed significant different associations between CTQ and

volumes in these regions between TT and GT carriers ($p_{\text{corrected}} < 0.01$) (detailed statistics provided in **Supplementary Table 3**). No significant main and genotype interaction effects of current stress (PSS) were observed for brain structure.

###Figure 1###

Interactive effects of TPH2 x CM on intrinsic network communication

CM and *TPH2* rs4570625 interactively impacted functional connectivity strengths between the left dACC and left DLPFC (MNI_{xyz} = [-6, 42, 27], $k = 24$, $p_{\text{FWE TFCE}} < 0.05$), with subsequent post-hoc tests demonstrating that the interaction was driven by pronounced effects of CM in the TT homozygotes, whereas both GT and GG groups did not show significant associations (TT: $r = -0.43$, $p_{\text{corrected}} = 0.0021$; GT: $r = 0.11$, $p = 0.27$; GG: $r = 0.20$, $p = 0.18$; centered at MNI_{xyz} = [-6, 42, 27]; Fisher's Z: $z_{\text{TT vs GT}} = 3.61$, $p < 0.001$; $z_{\text{TT vs GG}} = 3.47$, $p = 0.001$; $z_{\text{GT vs GG}} = 0$, $p = 1$) (**Fig. 2**). Given previously reported genotype-dependent effects of CM on amygdala activity (White et al., 2012) an amygdala-focused analysis (small-volume correction, SVC, AAL atlas amygdala) was employed which revealed interactive effects on left dACC - left amygdala functional connectivity (MNI_{xyz} = [-21, 0, -12], $k = 2$, $p_{\text{FWE}} < 0.05$) (**Fig. 2**). The interaction was driven by a pronounced effect of CM on left dACC - left amygdala connectivity in TT homozygotes, whereas GT and GG groups did not show significant associations (TT: $r = -0.34$, $p_{\text{corrected}} = 0.032$, GT: $r = 0.28$, $p_{\text{corrected}} = 0.055$; GG: $r = -0.14$, $p = 0.35$; Fisher's Z: $z_{\text{TT vs GT}} = 3.93$, $p < 0.001$; $z_{\text{TT vs GG}} = 1.136$, $p = 0.26$; $z_{\text{GT vs GG}} = 2.31$, $p = 0.021$) (**Fig. 2**). No significant interactive effects were observed with respect to the other seed regions.

No significant main and genotype interaction effects of current stress (PSS) were observed.

###Figure 2###

Associations with anxious avoidant behavior

The moderation analysis revealed a significant moderation effect ($R^2 = 0.05$, $F_{(4, 224)} = 3.12$, $p = 0.016$) reflecting that the interaction between CTQ and *TPH2* rs4570625 significantly predicts punishment sensitivity ($B = 0.094$, $SE = 0.044$, $t_{(224)} = 2.15$, $p = 0.03$). Genotype thus significantly moderated the association between CM and punishment sensitivity, with post hoc tests indicating that higher CM selectively associated with higher punishment sensitivity in TT carriers ($t_{(224)} = 2.59$, $p = 0.01$, **Fig. 3**, for visualization Johnson-Neyman approach was employed, splitting CTQ scores into low, medium, high).

###Figure 3###

Non-parametric correlation analysis revealed that specifically in TT homozygotes sensitivity to punishment was significantly positively associated with volumes of the thalamic-limbic region, right vmPFC and left DLPFC (right vmPFC: $r = 0.359$, $p_{\text{corrected}} = 0.006$; left DLPFC: $r = 0.387$, $p_{\text{corrected}} = 0.008$; bilateral thalamic-limbic: $r = 0.370$, $p_{\text{corrected}} = 0.026$) (**Fig. 4**, details see **Supplementary Table 3**). Associations between sensitivity to punishment and

left dACC connectivity failed to reach significance ($p_{\text{corrected}} > 0.05$) and thus was not further examined in the mediation.

###Figure 4###

The mediation model for brain volumes reached significance in the TT group only, implying individual variations in sensitivity to punishment may be explained by the level of CM exposure in the TT group. A significant overall indirect effect was observed (mediation by brain volume; indirect effect ratio, 66.75%; effect size $a \times b = 0.1096$, 95% confidence interval = [0.0247-0.2212]; $p < 0.05$), suggesting that thalamic-limbic-prefrontal volumes mediated the influence of CM on sensitivity to punishment in TT carriers (**Supplementary Table 4**).

Discussion

Previous animal models and initial findings in humans suggest that variations in serotonergic signaling associated with individual differences *TPH2* polymorphisms mediate the effects of early adverse experiences on emotional dysregulations (Forssman et al., 2014; Mandelli et al., 2012; Sachs et al., 2013). The present study found that *TPH2* rs4570625 genotype and CM interact to shape the structural and functional architecture of thalamic-limbic-prefrontal circuits, specifically in TT homozygotes higher CM exposure associates with increased volumes of hippocampal-amygda, thalamic and frontal regions and decreased functional connectivity between left dACC and left DLPFC, left amygdala, respectively whereas no associations were observed in the G-carrier groups. Moreover, *TPH2* genotype significantly moderated the impact

of CM on punishment sensitivity and in TT homozygotes higher levels of sensitivity to punishment were associated with both, higher exposure to CM and limbic and brain volumes. An additional mediation analysis furthermore suggests that increased brain volumes in this circuitry critically mediate the impact of aversive childhood experiences on sensitivity to punishment in TT carriers.

Most previous studies that did not account for genetic differences reported that higher CM associated with decreased brain volumes in limbic and prefrontal regions (Teicher et al., 2016). An additional analysis that pooled the G-carriers of the present sample revealed a negative association between CM and brain volumes in the pooled G-carrier group partly replication the previous findings (**Supplementary Table 5**). Animal models suggest that prolonged stress during sensitive developmental periods detrimentally impacts dendritic growth in limbic and prefrontal regions (Yang et al., 2015) which could partially explain lower volumes observed on the macro-anatomic level (Ivy et al., 2010). The few previous studies that examined whether polymorphisms modulate the impact of CM on brain structure in humans observed that specific allelic variants coding brain-derived neurotrophic growth factor and oxytocinergic pathways pathway genes exhibit pronounced volumetric decreases following CM (Dannlowski et al., 2016; van Velzen et al., 2016).

The observed opposite association between higher CM and increased brain volumes observed in the *TPH2* rs4570625TT homozygotes contrasts with these previous reports on a genetic susceptibility for pronounced CM-associated brain structural deficits. While some studies that combined the low-frequency *TPH2* rs4570625 T-carrier groups initially revealed increased psychopathological risk (Gao et al., 2012), anxiety-associated traits (Gutknecht et al.,

2007) and detrimental effects of CM (Forssman et al., 2014; Mandelli et al., 2012), accumulating evidence indicates that TT homozygotes differ from both other variants in terms of lower anxiety-related behavior and psychopathological risk (Ottenhof et al., 2018). While reduced gray matter volumes in limbic-prefrontal regions have been consistently reported in psychiatric disorders characterized by exaggerated anxiety and deficient emotion regulation (Bora, Fornito, Pantelis, & Yücel, 2012), associations between emotional functioning and limbic-prefrontal volumes in healthy subjects remain less clear, such that elevated anxiety has been associated with both, volumetric increases as well as decreases in this circuitry (e.g. Günther et al., 2018). On the other hand, a growing number of studies consistently reported positive associations between aversive learning and volumetric indices in this circuit (e.g. Hartley, Fischl, & Phelps, 2011) and trauma exposure in adulthood has been associated with volumetric increases of the amygdala and concomitantly facilitated aversive learning (Cacciaglia et al., 2017). In the present study, both, childhood aversive experience and thalamic-limbic-prefrontal volumes were positively associated with higher punishment sensitivity in the TT homozygotes. According to the reinforcement sensitivity theory, individual differences in trait punishment sensitivity are neutrally underpinned by the BIS, a brain-behavioral system that facilitates the formation of aversive motivation by orchestrating behavior in response to conditioned aversive events (Gray, 1987; Gray & McNaughton, 2000) and interacts with associative learning to facilitate aversive learning and future avoidance of threats (Reynolds, Askew, & Field, 2018). Increased punishment sensitivity on the phenotype level is considered to reflect an underlying hyperactive BIS system and has been consistently associated with better threat detection and facilitated aversive and avoidance learning (Avila & Parcet, 2000). The

identified network exhibiting genotype x CM exposure interaction effects highly overlaps with the neural circuits engaged in these functional domains, specifically the acquisition and extinction of conditioned threat responses (Milad & Quirk, 2012). Within this circuitry, the amygdala, hippocampus and dACC detect and encode threat probability of stimuli in the environment (e.g. Rodrigues, LeDoux, & Sapolsky, 2009) and are regulated by prefrontal-thalamic-limbic circuits that subserve implicit and explicit regulation of the innate or acquired threat response (Kalisch, 2009; Ramanathan, Jin, Giustino, Payne, & Maren, 2018). Serotonin plays an important role in these aversive learning mechanisms and underpins neuroplasticity in limbic-prefrontal circuits (Lesch & Waider, 2012). Mice with a knockin mutilated *TPH2* polymorphism (rs4570625) resulting in serotonin deficiency exhibit a phenotype characterized by facilitated threat reactivity and threat acquisition that are mediated by neural morphology in limbic regions, particularly the hippocampal-amygdalar complex (Waider et al., 2019).

Although the neurobiological implications of the *TPH2* rs4570625 polymorphism are not fully understood and the T-variant has been associated with increased as well as decreased central serotonergic transmission in limbic-prefrontal circuits (Ottenhof et al., 2018; Zhang et al., 2004; Lin et al., 2007 for Han population), the present findings may reflect that the *TPH2* rs6570625 polymorphism, perhaps reflecting individual differences in 5HT neurotransmission, may mediate the impact of CM via experience-dependent neuroplastic changes in thalamic-limbic-prefrontal circuits engaged in aversive learning. This may reflect that this polymorphism interacts with aversive environmental factors to shape a neural and behavior phenotype with an enhanced capability to detect and avoid threat and thus facilitating survival in a malevolent environment (Teicher et al., 2016).

On the network level, CM-associated volumetric increases observed in TT carriers were accompanied by decreased functional communication of the dACC with both, the DLPFC and the amygdala. Deficient intrinsic functional interaction within this circuit has been increasingly reported following CM and has been associated with increased emotional dysregulations and threat reactivity on the behavioral level (Kaiser et al., 2018). Deficient recruitment of the dACC and functional communication within the dACC-DLPFC-amygdala circuitry have been associated with impaired voluntary emotion regulation (Zilverstand, Parvaz, & Goldstein, 2017; Zimmermann et al., 2017). In this context, the present findings may suggest that the increased regional-specific volumes of the aversive learning circuit in TT carriers come at the expense of less regulatory control within this circuitry, shifting the systems towards higher sensitivity for threatening stimuli in the environment rather than internal emotion regulation. These alterations may reflect experience-dependent adaptations that promote avoidance of further harm in a malevolent childhood environment however may render individuals at an increased (latent) psychopathological vulnerability in adulthood. Although individuals with psychiatric diagnosis were not enrolled in the present study TT carriers reported slightly elevated levels of perceived current stress possibly reflecting elevated threat reactivity or deficient emotion regulation respectively. Alterations in these domains have been associated with aberrant amygdala-frontal functional connectivity that normalize with symptom-reduction in stress-related disorders (Spengler et al., 2017). Behavioral interventions and neuromodulatory strategies have been shown to facilitate emotion regulation via modulating amygdala-prefrontal connectivity (Zhao et al., 2019) and may have the potential as

promosing early interventions to alleviate increased psychopathlogical vulnerability following CM.

By capitalizing on the regulatory role of a common *TPH2* SNP on central serotonergic neurotransmission in combination with MRI and trait assessments in a representative sample of healthy subjects, the present study allowed us to determine the role of polymorphic gene differences presumably affecting serotonergic signaling on adaptation to early life stress on the neural and phenotype level. Owing to the low prevalence of the T-allele in Caucasian populations, previous studies combined T-carriers (Markett et al., 2016), whereas the higher frequency of the T-variant in Asian populations enabled us to additionally examine characteristics of the TT-homozygote variant. Nevertheless, the current findings need to be tempered by the following limitations: (1) Early life stress was retrospectively assessed; however, the reported level of CM did not differ between the genotype groups, and, (2) different effects of CM during different developmental periods have been reported, however, the retrospective assessment does not allow to further determine genotype-dependent differences in the onset of stress exposure.

Together, the present findings suggest that CM shapes the neural organization of the thalamic-limbic-prefrontal circuits in interaction with individual genetic variations in a *TPH2* polymorphism. The identified network strongly overlaps with the circuitry engaged in aversive learning and avoidant behavior. Previous studies suggest that serotonin facilitates aversive learning via promoting neuroplasticity in thalamic-limbic-prefrontal circuits. Within this context the present findings suggest that genetic differences in serotonergic signaling associated with a specific *TPH2* polymorphism determine the impact of early life aversive experiences on

the structural and functional architecture of the brain and shape a phenotype adapted to avoid threat in a malevolent environment.

Acknowledgments

This work was supported by the National Key Research and Development Program of China (2018YFA0701400); National Natural Science Foundation of China (91632117, 31530032); Open Research Fund of the State Key Laboratory of Cognitive Neuroscience and Learning, Beijing Normal University; Science, Innovation and Technology Department of the Sichuan Province (2018JY0001).

Conflict of interest statement The authors declare no conflict of interest

References

Avila, C., & Parcet, M. A. (2000). The role of Gray's impulsivity in anxiety - mediated differences in resistance to extinction. *European Journal of Personality, 14*(3), 185-198.

Birn, R. M., Roeber, B. J., & Pollak, S. D. (2017). Early childhood stress exposure, reward pathways, and adult decision making. *Proceedings of the National Academy of Sciences, 114*(51), 13549-13554.

Bora, E., Fornito, A., Pantelis, C., & Yücel, M. (2012). Gray matter abnormalities in major depressive disorder: a meta-analysis of voxel based morphometry studies. *Journal of affective disorders, 138*(1-2), 9-18.

Cacciaglia, R., Nees, F., Grimm, O., Ridder, S., Pohlack, S. T., Diener, S. J., . . . Flor, H. (2017). Trauma exposure relates to heightened stress, altered amygdala morphology and deficient extinction learning: implications for psychopathology. *Psychoneuroendocrinology, 76*, 19-28.

Cohen, S., Kamarck, T., & Mermelstein, R. (1983). A global measure of perceived stress. *Journal of health and social behavior, 24*, 385-396.

Dannlowski, U., Kugel, H., Grotegerd, D., Redlich, R., Opel, N., Dohm, K., . . . Suslow, T. (2016). Disadvantage of social sensitivity: interaction of oxytocin receptor genotype and child maltreatment on brain structure. *Biological psychiatry, 80*(5), 398-405.

Forssman, L., Peltola, M. J., Yrttiaho, S., Puura, K., Mononen, N., Lehtimäki, T., & Leppänen, J. M. (2014). Regulatory variant of the TPH 2 gene and early life stress are

associated with heightened attention to social signals of fear in infants. *Journal of Child Psychology and Psychiatry*, 55(7), 793-801.

Fung, B. J., Qi, S., Hassabis, D., Daw, N., & Mobbs, D. (2019). Slow escape decisions are swayed by trait anxiety. *Nature human behaviour*, 3, 702-708.

Günther, V., Ihme, K., Kersting, A., Hoffmann, K.-T., Lobsien, D., & Suslow, T. (2018). Volumetric associations between amygdala, nucleus accumbens, and socially anxious tendencies in healthy women. *Neuroscience*, 374, 25-32.

Gao, J., Pan, Z., Jiao, Z., Li, F., Zhao, G., Wei, Q., . . . Evangelou, E. (2012). TPH2 gene polymorphisms and major depression—a meta-analysis. *PloS one*, 7(5), e36721.

Gray, J., & McNaughton, N. (2000). Fundamentals of the septo-hippocampal system. *The Neuropsychology of Anxiety: An Enquiry into the Functions of Septo-hippocampal System*, 2nd ed. Oxford University Press, Oxford, 204-232.

Gray, J. A. (1987). *The psychology of fear and stress* (Vol. 5): CUP Archive.

Gutknecht, L., Jacob, C., Strobel, A., Kriegebaum, C., Müller, J., Zeng, Y., . . . Reif, A. (2007). Tryptophan hydroxylase-2 gene variation influences personality traits and disorders related to emotional dysregulation. *International Journal of Neuropsychopharmacology*, 10(3), 309-320.

Hartley, C. A., Fischl, B., & Phelps, E. A. (2011). Brain structure correlates of individual differences in the acquisition and inhibition of conditioned fear. *Cerebral Cortex*, 21(9), 1954-1962.

Ivy, A. S., Rex, C. S., Chen, Y., Dubé, C., Maras, P. M., Grigoriadis, D. E., . . . Baram, T. Z. (2010). Hippocampal dysfunction and cognitive impairments provoked by chronic

early-life stress involve excessive activation of CRH receptors. *Journal of Neuroscience*, 30(39), 13005-13015.

Kaiser, R., Clegg, R., Goer, F., Pechtel, P., Beltzer, M., Vitaliano, G., . . . Pizzagalli, D. (2018). Childhood stress, grown-up brain networks: corticolimbic correlates of threat-related early life stress and adult stress response. *Psychological medicine*, 48(7), 1157-1166.

Kalisch, R. (2009). The functional neuroanatomy of reappraisal: time matters. *Neuroscience & Biobehavioral Reviews*, 33(8), 1215-1226.

Lesch, K.-P., & Waider, J. (2012). Serotonin in the modulation of neural plasticity and networks: implications for neurodevelopmental disorders. *Neuron*, 76(1), 175-191.

Lin, Y.-M. J., Chao, S.-C., Chen, T.-M., Lai, T.-J., Chen, J.-S., & Sun, H. S. (2007). Association of functional polymorphisms of the human tryptophan hydroxylase 2 gene with risk for bipolar disorder in Han Chinese. *Archives of general psychiatry*, 64(9), 1015-1024.

Mandelli, L., Antypa, N., Nearchou, F. A., Vaiopoulos, C., Stefanis, C. N., Serretti, A., & Stefanis, N. C. (2012). The role of serotonergic genes and environmental stress on the development of depressive symptoms and neuroticism. *Journal of affective disorders*, 142(1-3), 82-89.

Markett, S., de Reus, M. A., Reuter, M., Montag, C., Weber, B., Schoene-Bake, J.-C., & van den Heuvel, M. P. (2016). Serotonin and the Brain's Rich Club—Association Between Molecular Genetic Variation on the TPH2 Gene and the Structural Connectome. *Cerebral Cortex*, 27(3), 2166-2174.

Milad, M. R., & Quirk, G. J. (2012). Fear extinction as a model for translational neuroscience: ten years of progress. *Annual review of psychology*, 63, 129-151.

Ottenhof, K. W., Sild, M., Lévesque, M. L., Ruhé, H. G., & Booij, L. (2018). TPH2 polymorphisms across the spectrum of psychiatric morbidity: A systematic review and meta-analysis. *Neuroscience & Biobehavioral Reviews*, 92, 29-42.

Preacher, K. J., & Hayes, A. F. (2004). SPSS and SAS procedures for estimating indirect effects in simple mediation models. *Behavior research methods, instruments, & computers*, 36(4), 717-731.

Preacher, K. J., & Hayes, A. F. (2008). Asymptotic and resampling strategies for assessing and comparing indirect effects in multiple mediator models. *Behavior research methods*, 40(3), 879-891.

Ramanathan, K. R., Jin, J., Giustino, T. F., Payne, M. R., & Maren, S. (2018). Prefrontal projections to the thalamic nucleus reuniens mediate fear extinction. *Nature communications*, 9(1), 4527.

Reynolds, G., Askew, C., & Field, A. P. (2018). Behavioral Inhibition and the Associative Learning of Fear *Behavioral Inhibition* (pp. 263-282): Springer.

Rodrigues, S. M., LeDoux, J. E., & Sapolsky, R. M. (2009). The influence of stress hormones on fear circuitry. *Annual review of neuroscience*, 32, 289-313.

Sachs, B. D., Rodriguez, R. M., Siesser, W. B., Kenan, A., Royer, E. L., Jacobsen, J. P., . . . Caron, M. G. (2013). The effects of brain serotonin deficiency on behavioural disinhibition and anxiety-like behaviour following mild early life stress. *International Journal of Neuropsychopharmacology*, 16(9), 2081-2094.

Sonuga-Barke, E. J., Kennedy, M., Kumsta, R., Knights, N., Golm, D., Rutter, M., . . .

Kreppner, J. (2017). Child-to-adult neurodevelopmental and mental health trajectories after early life deprivation: the young adult follow-up of the longitudinal English and Romanian Adoptees study. *The Lancet*, 389(10078), 1539-1548.

Spengler, F. B., Becker, B., Kendrick, K. M., Conrad, R., Hurlemann, R., Schade, G. (2017). Emotional dysregulation in psychogenic voice loss. *Psychotherapy and Psychosomatics*, 86(2), 121-123.

Teicher, M. H., Samson, J. A., Anderson, C. M., & Ohashi, K. (2016). The effects of childhood maltreatment on brain structure, function and connectivity. *Nature reviews neuroscience*, 17(10), 652-666.

Torrubia, R., Avila, C., Moltó, J., & Caseras, X. (2001). The Sensitivity to Punishment and Sensitivity to Reward Questionnaire (SPSRQ) as a measure of Gray's anxiety and impulsivity dimensions. *Personality and Individual Differences*, 31(6), 837-862.

van Velzen, L. S., Schmaal, L., Jansen, R., Milaneschi, Y., Opmeer, E. M., Elzinga, B. M., . . . Penninx, B. W. (2016). Effect of childhood maltreatment and brain-derived neurotrophic factor on brain morphology. *Social cognitive and affective neuroscience*, 11(11), 1841-1852.

Waider, J., Popp, S., Mlinar, B., Montalbano, A., Bonfiglio, F., Aboagye, B., . . . Araragi, N. (2019). Serotonin deficiency increases context-dependent fear learning through modulation of hippocampal activity. *Frontiers in neuroscience*, 13, 245.

White, M. G., Bogdan, R., Fisher, P. M., Munoz, K., Williamson, D. E., & Hariri, A. R. (2012). FKBP5 and emotional neglect interact to predict individual differences in amygdala reactivity. *Genes, Brain and Behavior*, 11(7), 869-878.

Winkler, A. M., Ridgway, G. R., Webster, M. A., Smith, S. M., & Nichols, T. E. (2014). Permutation inference for the general linear model. *Neuroimage*, 92, 381-397.

Yang, X.-D., Liao, X.-M., Uribe-Marino, A., Liu, R., Xie, X.-M., Jia, J., . . . Wang, X.-D. (2015). Stress during a critical postnatal period induces region-specific structural abnormalities and dysfunction of the prefrontal cortex via CRF 1. *Neuropsychopharmacology*, 40(5), 1203-1215.

Zhang, X., Beaulieu, J.-M., Sotnikova, T. D., Gainetdinov, R. R., & Caron, M. G. (2004). Tryptophan hydroxylase-2 controls brain serotonin synthesis. *Science*, 305(5681), 217-217.

Zhao, Y., Yao, S., Li, K., Sindermann, C., Zhou, F., Zhao, W., . . . Becker, B. (2019). Real-time functional connectivity-informed neurofeedback od amygdala-frontal pathways reduces anxiety. *Psychotherapy and Psychosomatics*, 88(1), 5-15.

Zilverstand, A., Parvaz, M. A., & Goldstein, R. Z. (2017). Neuroimaging cognitive reappraisal in clinical populations to define neural targets for enhancing emotion regulation. A systematic review. *Neuroimage*, 151, 105-116.

Zimmermann, K., Walz, C., Derckx, R. T., Kendrick, K. M., Weber, B., Dore, B., . . . Becker, B. (2017). Emotion regulation deficits in regular marijuana users. *Human brain mapping*, 38(8), 4270-4279.

Table 1. Sample characteristics (n = 229) stratified according to *TPH2* rs4570625

	TT (n = 71)	GT (n = 107)	GG (n = 51)	p Value
Age, Years	21.55 ±2.48	21.46 ±2.24	21.76 ±2.27	0.74 ^a
Gender (M/F)	32/39	56/51	26/25	0.63 ^b
Education, Years	15.55 ±2.09	15.69 ±1.84	15.78 ±1.84	0.79 ^a
CTQ	38.08 ±9.22	37.92 ±10.65	38.45 ±9.10	0.95 ^a
PSS	26.18 ±5.51	23.61 ±5.38	24.55 ±5.21	0.008 ^a
SPS	11.11 ±4.81	10.21 ±4.49	10.96 ±3.79	0.363 ^a

Mean and standard deviations ($\pm SD$) are displayed. Abbreviations: CTQ, Childhood Trauma Questionnaire; F, female; M, male; PSS, Perceived Stress Scale; SPS, Sensitivity to Punishment scale. ^a*F* tests, ^b χ^2 tests

Figures and captions to figures

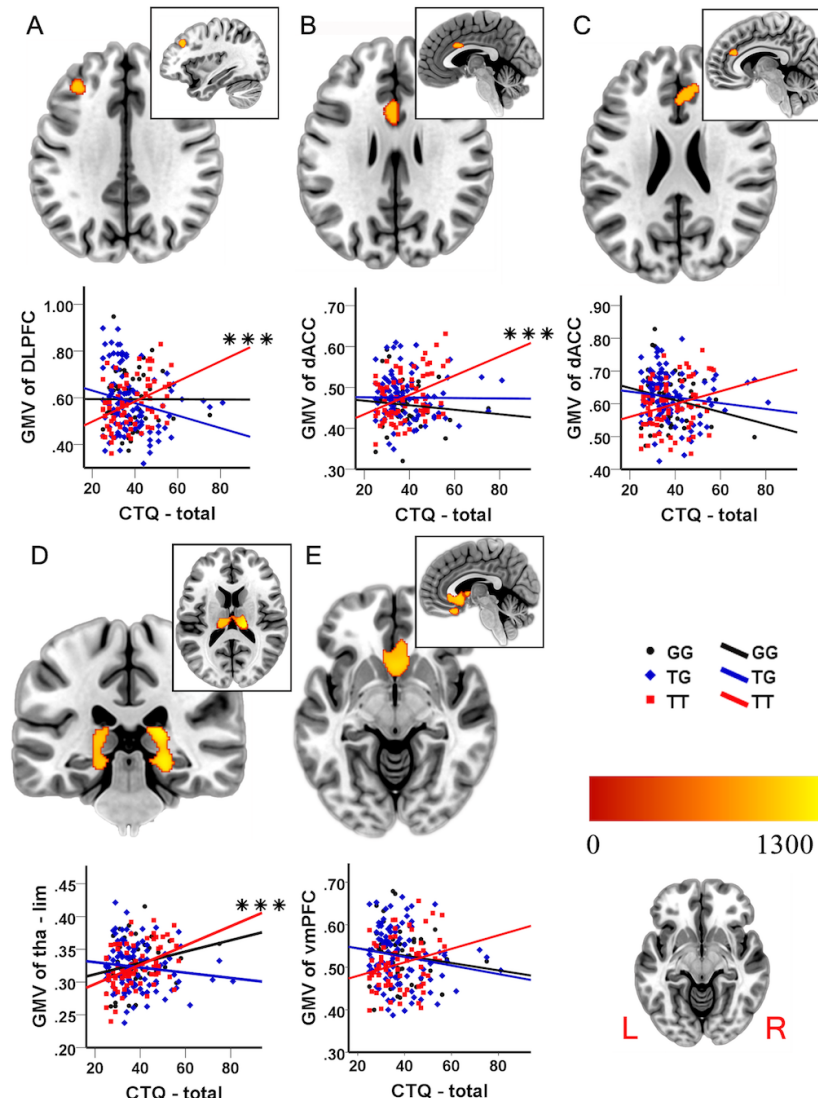


Fig. 1. Interaction of *TPH2* rs4570625 and ELS on grey matter structure and relationship

between grey matter volume and Childhood-Trauma -Questionnaire (CTQ) scores. Regions

showing significant interaction effects between genotype and early life stress (color bar = TFCE

value, p_{FWE} with TFCE < 0.05) (2A-2E).

dACC, dorsal anterior cingulate cortex; vmPFC, ventromedial frontal cortex; DLPFC,

dorsolateral prefrontal cortex; thalamic-limbic, parahippocampus/hippocampus/

amygdala/thalamus; *** $p < 0.001$, Bonferroni-corrected

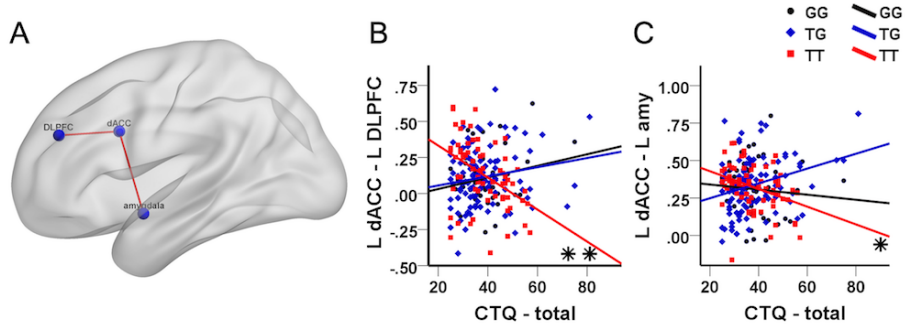


Fig. 2. Interaction of *TPH2* rs4570625 and ELS on the functional connectivity strength of the left dorsal anterior cingulate cortex (dACC) (3A). Associations between extracted parameter estimates and CTQ total scores for dACC – left DLPFC (3B) left amygdala (3C).
dACC, dorsal anterior cingulate cortex; DLPFC, dorsolateral prefrontal cortex; amy, amygdala;

* $p < 0.05$; ** $p < 0.01$, Bonferroni-corrected

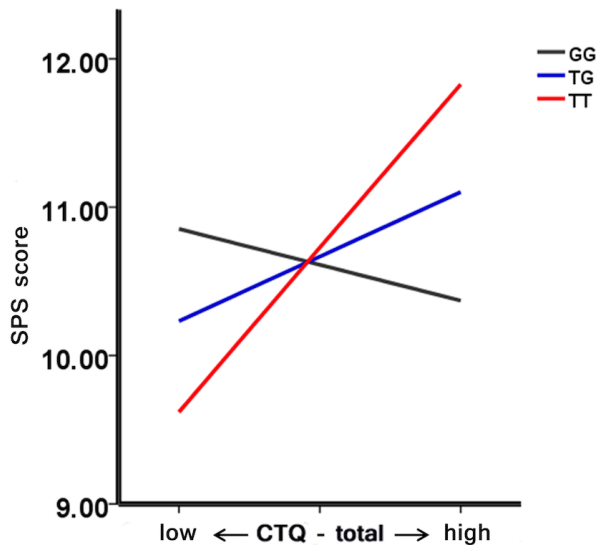


Fig. 3. Moderation effect of genotype on the association between sensitivity to punishment scale (SPS) and Childhood Trauma Questionnaire (CTQ) scores.

SPS, sensitivity to punishment scale; CTQ, Childhood Trauma Questionnaire.

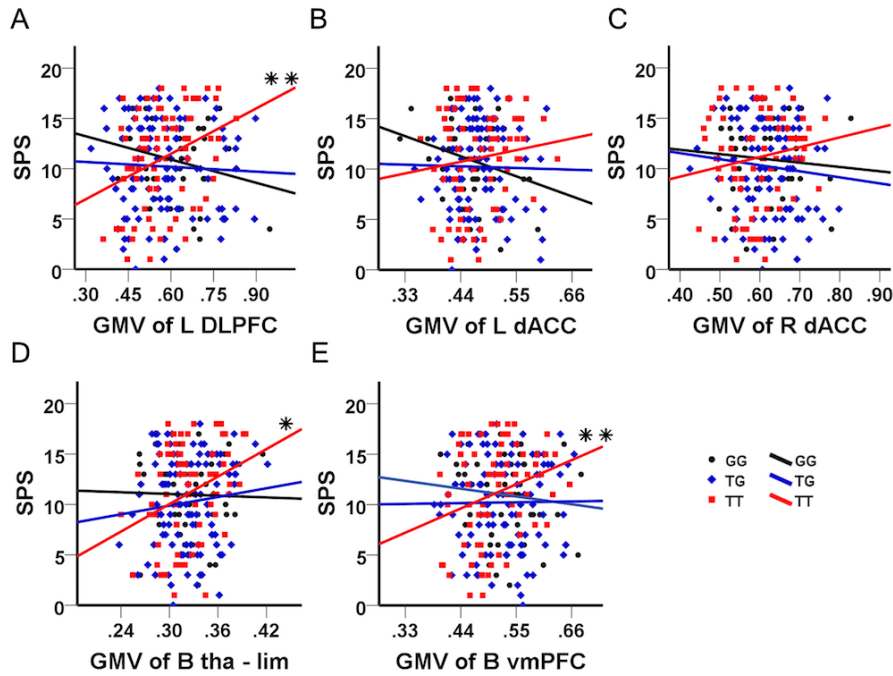


Fig. 4. Relationship between gray matter volume and sensitivity to punishment scale (SPS)

scores for TT homozygotes (red), TG heterozygotes (blue) and GG homozygotes (black) in the regions showing significant genotype x early life stress effects (5A-D).

GMV, gray matter volume; dACC, dorsal anterior cingulate cortex; vmPFC, ventromedial frontal cortex; DLPFC, dorsolateral prefrontal cortex; thalamic-limbic, parahippocampus gyrus/ hippocampus/thalamus; L, left; R, right; B, bilateral; * $p < 0.05$; ** $p < 0.01$, Bonferroni-corrected

Supplementary Information

Authors Congcong Liu et al.

Correspondence Benjamin Becker (ben_becker@gmx.de)

Supplementary methods

MRI data acquisition

MRI data acquisition was conducted on a 3.0 Tesla GE MR750 system (General Electric Medical System, Milwaukee, WI, USA). T1-weighted high-resolution anatomical images were acquired with a spoiled gradient echo pulse sequence, repetition time (TR) = 5.9 ms, echo time (TE) = minimum, flip angle = 9°, field of view (FOV) = 256 × 256 mm, acquisition matrix = 256 × 256, thickness = 1 mm, number of slice = 156. For the resting state, a total of 210 functional volumes were acquired using a T2*-weighted Echo Planar Imaging (EPI) sequence (TR = 2000 ms, TE = 30 ms, FOV = 240 × 240 mm, flip angle = 90°, image matrix = 64 × 64, thickness/gap = 3.4/0.6mm, 39 axial slices with an interleaved ascending order). During the resting-state acquisition, participants were instructed to lie still and to fixate a white cross centered on a black background while not falling asleep. In post-MRI interviews, none of the subjects reported having fallen asleep during the scan. OptoActive MRI headphones (<http://www.optoacoustics.com/>) were used to reduce acoustic noise exposure during MRI acquisition (Roozen, Koevoets, & Den Hamer, 2008).

Preprocessing brain structural data

T1-weighted anatomical images were initially visually inspected to verify absence of

anatomical abnormalities and image quality, and next manually reoriented to the anterior commissure – posterior commissure (AC-PC). The structural images were subsequently preprocessed using SPM12 (Statistical Parametric Mapping, <http://www.fil.ion.ucl.ac.uk/spm/>). The brain volumes were first segmented into gray matter (GM), white matter (WM) and cerebrospinal fluid (CSF) using the new unified segmentation approach (Ashburner & Friston, 2005; Malone et al., 2015). Second, a group-specific template based on all participants was created using DARTEL algorithm (Ashburner, 2007). Next, the segmented GM and WM images were iteratively registered via the fast diffeomorphic registration DARTEL algorithm to warp the GM and WM partitions on to the template and subsequently non-linearly normalized to MNI space. Finally, gray matter volumes were spatially smoothed with a Gaussian 8 mm FWHM (full width at half maximum) kernel. Total intracranial volume (TIV) was estimated and used as a covariate on the second level.

Preprocessing resting state functional MRI data

To examine whether the regional brain structural alterations were accompanied by functional communication differences between the nodes, resting state data was additionally acquired. Resting-state functional time-series were preprocessed using SPM12. For each subject, the first ten volumes were discarded to allow for T1 equilibration effect and allow active noise cancelling by the headphones. The remaining functional images were slice-time corrected and realigned to the first image to correct for head motion. The EPI images were then co-registered to the T1-weighted structural images, normalized to Montreal Neurological

Institute (MNI) standard space using the segmentation parameters from the structural images and interpolated to $3 \times 3 \times 3$ mm voxel size. Normalized images were finally spatially smoothed with a 6 mm FWHM. Next, 24 head movement parameters (i.e., 6 head motion parameters, 6 head motion parameters one time point before, and the 12 corresponding squared items) (Friston, Williams, Howard, Frackowiak, & Turner, 1996) along with mean signals from WM and CSF were removed from the data through linear regression. Finally, the influences of low-frequency drift and high-frequency noise were restricted by a band-pass filter (0.01–0.1 Hz). For the rsfMRI analyses, three subjects were excluded due to excessive head motion (exclusion criterion > 3 mm and/or 3 degrees, $n = 2$) or missed rsfMRI data ($n = 1$).

Functional connectivity analyses were performed using the Resting-State fMRI Data Analysis Toolkit (REST; <http://www.restfmri.net>). 5-mm spheres centered at the peak coordinates of significant clusters in the VBM analyses served as seed regions to create seed-to-whole brain intrinsic connectivity maps. To this end, the individual mean time series of each seed ROI was calculated and next correlation coefficients between the seed time series and other voxels were calculated to obtain r maps for each participant. Fisher z score transformations were employed to generate z -FC maps. Finally, z -FC maps were subjected to second-level random-effects group analyses. Consistent with the brain structural analyses, a single full factorial model was conducted using PALM with genotype group (TT vs GT vs GG) as between-subjects factor. CTQ scores were entered as covariate, including the interaction term of genotype and CTQ. Age, gender, education and mean framewise displacement (Van Dijk, Sabuncu, & Buckner, 2012) were included as nuisance regressors. All covariates were

mean-centered across participants.

References supplementary materials

Ashburner, J. (2007). A fast diffeomorphic image registration algorithm. *Neuroimage*, 38(1), 95-113.

Ashburner, J., & Friston, K. J. (2005). Unified segmentation. *Neuroimage*, 26(3), 839-851.

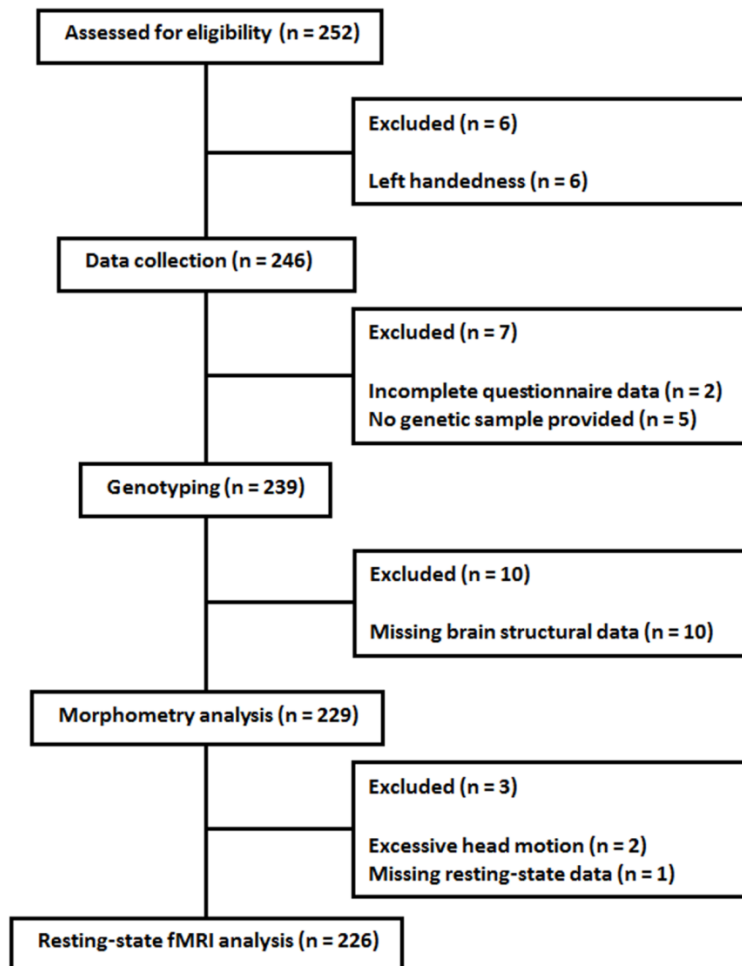
Friston, K. J., Williams, S., Howard, R., Frackowiak, R. S., & Turner, R. (1996). Movement - related effects in fMRI time - series. *Magnetic resonance in medicine*, 35(3), 346-355.

Malone, I. B., Leung, K. K., Clegg, S., Barnes, J., Whitwell, J. L., Ashburner, J., . . . Ridgway, G. R. (2015). Accurate automatic estimation of total intracranial volume: a nuisance variable with less nuisance. *Neuroimage*, 104, 366-372.

Roozen, N., Koevoets, A., & Den Hamer, A. (2008). Active vibration control of gradient coils to reduce acoustic noise of MRI systems. *IEEE/ASME Transactions on Mechatronics*, 13(3), 325-334.

Van Dijk, K. R., Sabuncu, M. R., & Buckner, R. L. (2012). The influence of head motion on intrinsic functional connectivity MRI. *Neuroimage*, 59(1), 431-438.

Supplementary figure 1 Flow diagram displaying exclusion of participant and rationale



Supplementary table 1

Interaction between *TPH2* genotype and ELS on brain structure (whole-brain)

Brain Area	Peak located at MNI			TFCE	Cluster Size k	$p_{\text{FWE with TFCE}}$
L dACC	-1.5	12	28.5	932.25	181	0.045
L DLPFC	-34.5	31.5	34.5	1008.65	201	0.034
B thalamic-limbic	19.5	-25.5	12	1238.10	2609	0.015
B vmPFC	1.5	15	-7.5	1068.18	1575	0.027
R dACC	6	33	24	956.25	335	0.042

Abbreviations: TFCE, threshold-free cluster enhancement; dACC, dorsal anterior cingulate cortex; vmPFC, ventromedial frontal cortex; DLPFC, dorsolateral prefrontal cortex; thalamic-limbic, parahippocampus gyrus/ hippocampus/thalamus/amygdala; L, left; R, right; B, bilateral; GMV, gray matter volume.

Supplementary table 2

Correlation between GMV and CTQ and correlation differences between genotypes

Brain Area	MNI coordinates			Genotype ^a			Z value ^a		
				GG	TG	TT	GG vs TG	GG vs TT	TG vs TT
	GG	TG	TT	GG vs TG	GG vs TT	TG vs TT			
L dACC	-1.5	12	28.5	0.00	-0.03	0.47***	0.19	2.71	3.48**
L DLPFC	-34.5	31.5	34.5	0.08	-0.27	0.49***	2.08	2.38	5.22***
B thalamic-limbic	19.5	-25.5	12	0.37	-0.15	0.47***	3.11*	0.65	4.26***
B vmPFC	1.5	15	-7.5	-0.03	-0.25	0.35	1.27	2.07	3.93**
R dACC	6	33	24	-0.12	-0.18	0.35	0.33	2.59	3.49**

Mean gray matter volumes were extracted from a 5-mm sphere centered at the peak coordinates of the respective clusters identified in the VBM analyses. Results were corrected for multiple comparisons using Bonferroni correction ^(a). Abbreviations: dACC, dorsal anterior cingulate cortex; vmPFC, ventromedial frontal cortex; DLPFC, dorsolateral prefrontal cortex; thalamic-limbic, parahippocampus gyrus/ hippocampus/thalamus /amygdala; L, left; R, right; GMV, gray matter volume; CTQ, Childhood Trauma Questionnaire. * $p < 0.05$; ** $p < 0.01$; *** $p < 0.001$.

Supplementary Table 3

Associations between gray matter volume and sensitivity to punishment

Brain Area	MNI coordinates	Genotype ^a			Z value ^b		
		GG	TG	TT	GG	GG	TG
					vs TG	vs TT	vs TT
L dACC	-1.5 12 28.5	-0.14	0.02	0.20	0.90	1.83	1.21
L DLPFC	-34.5 31.5 34.5	-0.12	-0.02	0.39**	0.62	2.83**	2.72**
B thalamic -limbic	19.5 -25.5 12	0.07	0.15	0.37*	0.46	1.68	1.51
B vmPFC	1.5 15 -7.5	0.07	0.06	0.36**	0.02	1.65	2.01*
R dACC	6 33 24	0.06	-0.05	0.24	0.65	0.96	1.89

Gray matter volumes extracted from regions demonstrating significant environment x genetic interactions and associations with punishment sensitivity. Positive associations were specifically observed in the TT homozygotes. Abbreviations: dACC, dorsal anterior cingulate cortex; vmPFC, ventromedial frontal cortex; DLPFC, dorsolateral prefrontal cortex; thalamic-limbic, parahippocampus gyrus/ hippocampus/thalamus/amygadala; L, left; R, right; B, bilateral; GMV, grey matter volume; SPS, sensitivity to punishment scale.

* $p < 0.05$; ** $p < 0.01$; *** $p < 0.001$; ^amultiple comparisons corrected with Bonferroni correction; ^bno Bonferroni-correction applied